

Carbaporphyrinoids Containing a Pyridine Moiety: 3-Aza-*meta*-benzporphyrin and 24-Thia-3-aza-*meta*-benzporphyrin

Radomir Myśluborski^[a] and Lechosław Latos-Grażyński^{*[a]}

Keywords: Porphyrin / Carbaporphyrinoid / Phlorin / Chlorin / Porphyrin

6,11,16,21-Tetraaryl-3-aza-*m*-benzporphyrin, an analog of 5,10,15,20-tetraarylporphyrin with one of the pyrrole units replaced by a pyridine ring pointing outwards, linked at β, β' positions, was formed by condensation of 3,5-bis[phenyl(2-pyrrolyl)methyl]pyridine, pyrrole and *p*-tolualdehyde catalyzed by TFA. The [3+1] approach, which involved a condensation of 3,5-bis[phenyl(2-pyrrolyl)methyl]pyridine with 2,5-bis[hydroxy(*p*-tolyl)methyl]thiophene was applied to afford 6,11,16,21-tetraaryl-24-thia-3-aza-*m*-benzporphyrin. Introduction of bulky substituents at *ortho* positions of *meso*-aryl compounds, adjacent to the pyridine ring, resulted in an increase in the yield of condensation. 3-Aza-*m*-benzporphyrins and 24-thia-3-aza-*m*-benzporphyrins have the ¹H NMR spectroscopic features of non-aromatic molecules. Crystal structures of 6,21-diphenyl-11,16-di-*p*-tolyl-3-aza-*m*-benzporphyrin and 6,21-diphenyl-11,16-di-*p*-tolyl-24-thia-3-aza-*m*-benzporphyrin were determined by X-ray crystallogra-

phy. Both molecules show a similar degree of nonplanarity with the pyridine ring sharply tipped out of the N(23)X(24)N(25) plane, making room for the 6,21-phenyl groups which are almost coplanar with the macrocycle. The protonation of 6,21-diphenyl-11,16-di-*p*-tolyl-3-aza-*m*-benzporphyrin with trifluoroacetic acid proceeds stepwise, subsequently yielding two dicationic and one tricationic species. Protonated 6,21-diphenyl-11,16-di-*p*-tolyl-24-thia-3-aza-*m*-benzporphyrin reacts reversibly with water to give 6-hydroxy-6,21-diphenyl-11,16-di-*p*-tolyl-24-thia-3-aza-*m*-benzporphlorin. The protonation of 6,21-dimesityl-11,16-di-*p*-tolyl-24-thia-3-aza-*m*-benzporphyrin initiates an unprecedented process, which converts the non-aromatic carbaporphyrinoid reversibly into the aromatic 2-hydroxy-6,21-dimesityl-11,16-di-*p*-tolyl-24-thia-3-aza-*m*-benzichlorin.

(© Wiley-VCH Verlag GmbH & Co. KGaA, 69451 Weinheim, Germany, 2005)

Introduction

Large families of expanded, contracted, and isomeric porphyrins were brought into existence by changing the number and sequence of the constituent pyrrole rings and carbon linkages.^[1,2] A group of modifications that we have found particularly interesting involves the introduction of C–H moieties into the coordination core of the porphyrin, so as to replace one or more of the pyrrolic nitrogen atoms. Such molecules, known as carbaporphyrinoids, offer the possibility of stabilizing rare types of metal–carbon bonds in a macrocyclic setting.^[3–7] The inner C–H unit of a carbaporphyrinoid is a part of carbocyclic or heterocyclic moieties. In the first group of carbaporphyrinoids the inner C–H bond belongs to a carbocyclic fragment,^[5] as exemplified by benzene in benzoporphyrins.^[8–12] Actually, various compounds of this type are known that incorporate different mono- and polycyclic moieties into their structures. The choice of the carbocycle affects the degree of π -conjugation in the system, and consequently the macrocyclic aromaticity in some carbaporphyrinoids is attenuated or totally absent. Alternatively, the CH fragment is provided by appropriately oriented five-membered heterocyclopentadienes

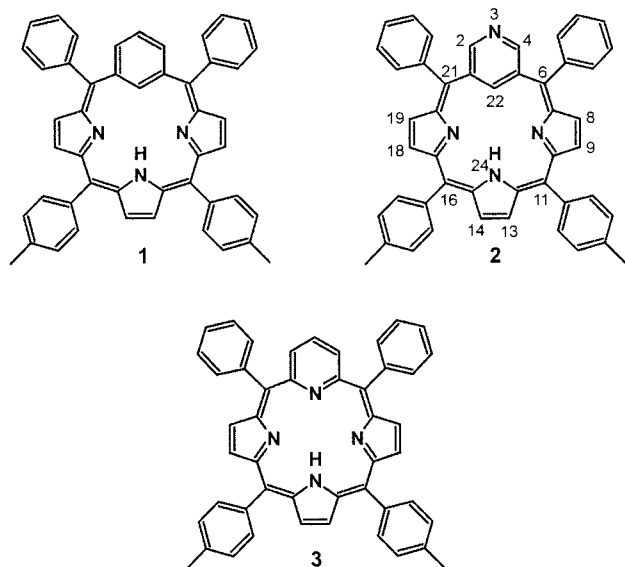
(pyrrole, furan, thiophene)^[13–18] to yield *N*-, *O*- or *S*-confused porphyrins, respectively. In this way the electronic structure of the porphyrin is profoundly altered leading to reactivity patterns that are unknown to the parent porphyrins or heteroporphyrins.

Recently, we have synthesized 6,11,16,21-tetraphenylbenzporphyrin (**1**), which can be formally constructed by replacement of one of the pyrrole rings of 5,10,15,20-tetraphenylporphyrin (TPP)H₂ with a *meta*-phenylene moiety.^[10] Benzoporphyrins are versatile ligands, which offer a means to study the metal–arene couple in a macrocyclic environment.^[6,10–12,19–21] The coordination brings the metal ion into the vicinity of the arene leading to activation of C–H bonds followed by dissociation and coordination or weak interactions, which can be spectroscopically observed.^[12]

Here, in search of a route to control the properties of benzoporphyrins we have synthesized 6,11,16,21-tetraaryl-3-aza-*m*-benzporphyrin (**2**). Formally this macrocycle has been constructed by replacement of one of the pyrrole rings of 5,10,15,20-tetraarylporphyrin with a pyridine moiety, linked to the macrocycle by the 3,5-carbon atoms. Alternatively, the molecule can be treated as a derivative of 6,11,16,21-tetraaryl-*m*-benzporphyrin (**1**) where the 3-CH fragment has been exchanged with the nitrogen atom to yield 6,11,16,21-tetraaryl-3-aza-*m*-benzporphyrin (**2**). As it is readily seen, by analogy to a porphyrin/*N*-confused por-

[a] Department of Chemistry, University of Wrocław, 14 F. Joliot-Curie St., Wrocław 50383, Poland
E-mail: LLG@wchuwr.chem.uni.wroc.pl

pyrrole couple, the 3-*aza-m*-benzporphyrin can be related to a regular pyriporphyrin **3** (22-*aza-m*-benzporphyrin) applying the *N*-confusion concept as shown in Scheme 1.



Scheme 1. *m*-Benzporphyrin and *aza-m*-benzporphyrins.

However, the regular pyriporphyrin (22-*aza-m*-benzporphyrin) **3** has not been synthesized until now, although the related, reduced macrocycle has been reported.^[22] The rearrangement of the *N*-substituted porphyrins in the presence of nickel(II) acetate resulted in the formation of a chlorin-like macrocycle, which contains a reduced pyridine fragment.^[23] The incorporation of 3-hydroxypyridine into the porphyrinic macrocycle results in the formation of 2-oxypyriporphyrin by a keto/enol tautomerization, which contains a pyridone moiety.^[24–27] The [4+1] condensation of tetrapyrrole and 3-hydroxypyridine-2,6-dicarboxaldehyde gave the sapphyrin derivative where the central pyrrole ring was replaced by 3-hydroxypyridine.^[28] The reaction of 2,6-dipyrrolylpyridine and benzaldehyde afforded dipyrhexaphyrin(1.0.0.1.0.0), containing two pyridine moieties, which replaced two central pyrrole rings of hexaphyrin(1.0.0.1.0.0).^[29,30] (Oxypyriporphyrin)nickel(II) was formed in the cyclization of (*vic*-dihydroxyoctaethylchlorin)-nickel(II) by secchlorin formation.^[31,32] Reaction of dichlorocarbene with *meso*-octamethylcalix[4]pyrrole caused pyrrole ring expansion, affording chlorocalixpyridinopyrroles and chlorocalixpyridines, which correspond to the porphyrinogen oxidation state.^[33]

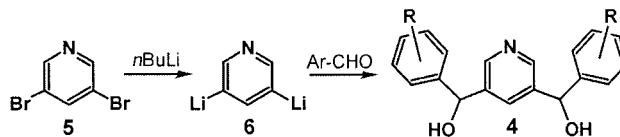
Paradoxically, the carbaporphyrinoid 6,11,16,21-tetraaryl-3-*aza-m*-benzporphyrin **2** is the very first “true” pyriporphyrin containing an unperturbed pyridine ring in the *N*-confused macrocyclic framework.

Results and Discussion

Synthesis

The key step in the synthesis of 6,11,16,21-tetraaryl-3-*aza-m*-benzporphyrin (**2**) is the construction of the conden-

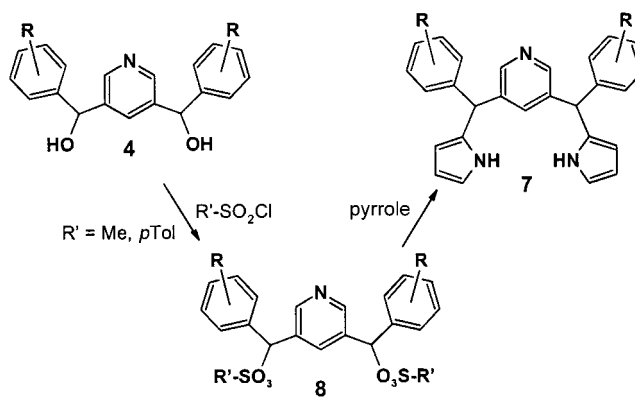
sation precursor, i.e. 3,5-bis[aryl(hydroxy)methyl]pyridine (**4**) (Scheme 2), which is a suitable synthon for introducing the *N*-confused pyridine ring into a porphyrin-like skeleton. The lithiation of 3,5-dibromopyridine (**5**), with *n*-butyllithium yielded the 3,5-dilithium derivative **6**.^[34] The lithiation step has been followed by reaction with benz- or mesitaldehydes, to convert **6** into the target molecules **4** or **4-M**, respectively (Scheme 2).



Scheme 2. Synthesis of 3,5-bis[aryl(hydroxy)methyl]pyridine **4**.

Typically, the condensation of pyrrole, arenealdehyde, 1,3-bis(arylhydroxymethyl)heterocyclopentadiene or 1,3-bis[aryl(hydroxy)methyl]benzene in the presence of $\text{BF}_3 \cdot \text{Et}_2\text{O}$ or TFA, resulted in the synthesis of tetraarylheteroporphyrin or tetraaryl-*m*-benzporphyrin, respectively.^[3,10,11] Contrary to our expectations the analogous procedure, using **4** as a substrate, has not produced any detectable amount of the targeted carbaporphyrinoid **2**. Presumably the substrate **4** has been deactivated by acidic catalysts as previously detected in syntheses of porphyrins containing *meso*-2/3/4-pyridyl substituents.^[35]

In order to overcome this problem the [3+1] strategy, frequently applied in the synthesis of β -substituted porphyrins,^[36] has been exploited. In such an approach 3,5-bis[aryl(2-pyrrolyl)methyl]pyridine (**7**) is the key compound as the “3” component of the condensation reaction (Scheme 3).

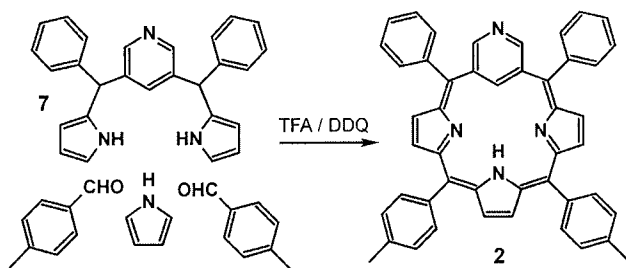


Scheme 3. Synthesis of 2,5-bis[aryl(2-pyrrolyl)methyl]pyridine **7**.

In a typical experiment, **4** is converted into **8**, i.e. the tosylate or mesylate derivatives of **7**. Compound **8** was not isolated but used directly in the next synthetic step. We found that it is necessary to replace the OH group in **4** by a better leaving group. The condensation of **4** with pyrrole to obtain **7** was unsuccessful. Contrary, the 45–90% yield of **7** or **7-M** has been achieved using the mesylate derivative **8** depending on aryl substitution.

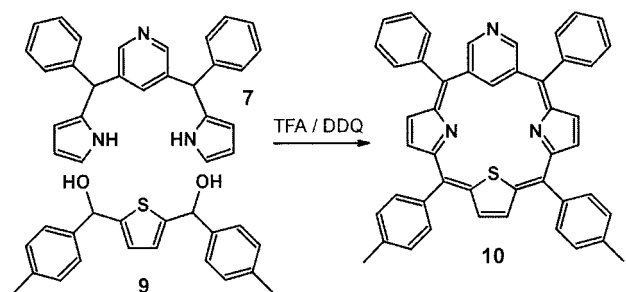
A condensation of 3,5-bis[2-pyrrolyl(phenyl)methyl]pyridine **7** with 1 equiv. of pyrrole and 6 equiv. of *p*-tolual-

dehyde in dichloromethane, catalyzed by TFA and followed by oxidation with DDQ, resulted in 6,21-diphenyl-11,16-di-*p*-tolyl-3-aza-*m*-benzporphyrin (**2**) (Scheme 4). After chromatographic workup and crystallization, **2** was obtained in 2.5% yield.



Scheme 4. Synthesis of **2**.

The rigorous [3+1] approach was applied to afford 6,21-diphenyl-11,16-di-*p*-tolyl-24-thia-3-aza-*m*-benzporphyrin (**10**) (Scheme 5). The condensation of 3,5-bis[phenyl(2-pyrrolyl)methyl]pyridine (**7**) with 2,5-bis[hydroxy(*p*-tolyl)methyl]thiophene (**9**) in dichloromethane, catalyzed by TFA and followed by oxidation with DDQ, resulted in **10** in 3% yield.



Scheme 5. Synthesis of **10**.

Analogous condensations have been carried out using 3,5-bis[mesityl(2-pyrrolyl)methyl]pyridine (**7-M**). Introduction of bulky substituents at *ortho* positions of *meso*-aryl groups, adjacent to the incorporated pyridine ring, increased the stability of **7** toward acidolysis during the condensation. The scrambling effect has been minimized and the unreacted compound **7-M** was observed after 6 h of condensation. Significantly, the rather modest structural change of **7** resulted in a remarkable increase in the yield of condensation [6,21-dimesityl-11,16-di-*p*-tolyl-3-aza-*m*-benzporphyrin (**2-M**), 15%; 6,21-dimesityl-11,16-di-*p*-tolyl-24-thia-3-aza-*m*-benzporphyrin (**10-M**), 18%].

Spectroscopic Studies

The electronic spectrum of **2** (Figure 1) demonstrates two bands at 411 nm and 700–760 nm resembling the spectroscopic features of non-aromatic 6,11,16,21-tetraphenylbenzporphyrin (**1**).^[10] The electronic spectrum of **10** resembles that of **2** but with a distinctive hypochromic shift of the low-energy band.

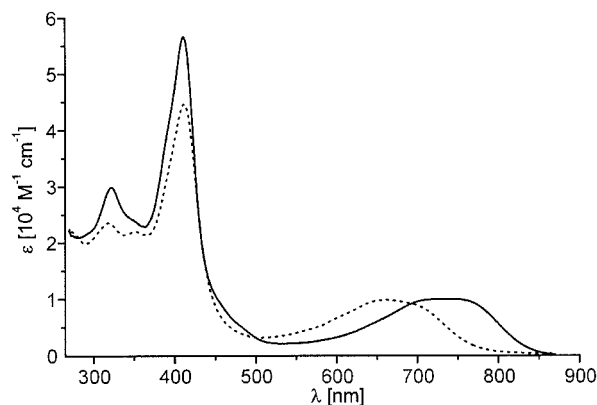


Figure 1. Electronic spectra of **2** (—) and **10** (···) in CH₂Cl₂.

For topological reasons the molecules **2** and **10** cannot retain the macrocyclic aromaticity typical of porphyrins. Thus, the ¹H NMR spectra of **2** and **10** show resonances at positions consistent with non-aromatic structures (Figure 2).

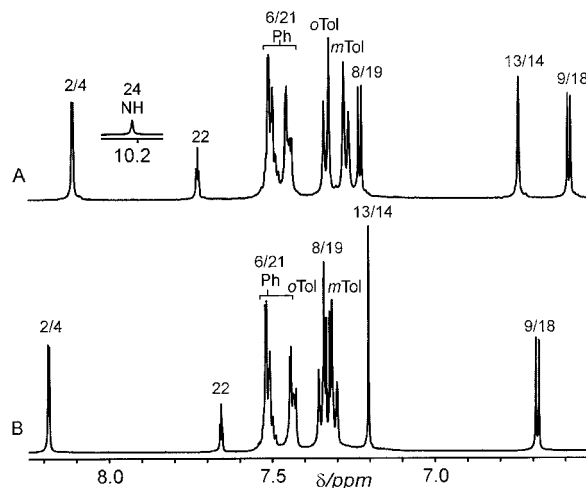


Figure 2. ¹H NMR spectra ([D₂]dichloromethane, 298 K) of **2** (A) and **10** (B). Resonance assignments (obtained from COSY and NOESY experiments) follow the numbering scheme given in Scheme 1.

The macrocyclic aromatic ring current is absent in **2**, clearly illustrated by the downfield shift of the NH(24) resonance ($\delta = 10.25$ ppm, [D₂]dichloromethane, 298 K) (Figure 2, trace A) and the positions of pyrrole and pyridine resonances, assigned by 2D experiments ($\delta = 7.24$ H(8/19), 6.59 H(9/18), 6.75 H(13/14), 8.11 H(2/4), 7.72 H(22) ppm, [D₂]dichloromethane, 298 K). Scalar coupling detected between the NH(24) and H(13/14) pyrrole protons is consistent with the prevalence of the symmetrical tautomer **2**. The NMR spectroscopic features of **10** resemble those of **2** ($\delta = 7.33$ H(8/19), 6.69 H(9/18), 7.21 H(13/14), 8.19 H(2/4), 7.66 H(22) ppm, [D₂]dichloromethane, 298 K). The marked difference between the H(8/19) and H(9/18) chemical shifts (ca. 0.6 ppm) is caused by the peculiar orientation of *meso* substituents as shown in the X-ray structures. Because of significant puckering of the macrocycle the 6/21-phenyl

rings are nearly coplanar with the macrocycle, which results in deshielding of the H(8/19) hydrogen atoms. An analogous difference of chemical shifts was recently reported for tetraaryl-*m*-benzporphyrin.^[10] The ¹H chemical shift values for the thiophene and pyrrole hydrogen atoms of **2** and **10** are in the range determined for other non-aromatic fully conjugated systems, which contain thiophene and pyrrole moieties.^[37] The pyridine moiety embedded in the macrocyclic structure shows similar chemical shifts to those seen for **4** or **7**.

The discussed ¹H and ¹³C NMR spectra of **2** and **10** correspond to an effectively planar structure contrary to the puckered structures observed in the solid state for free bases. This leads to the suggestion that 3-aza-*m*-benzporphyrin macrocycles, analogous with *m*- and *p*-benzporphyrins, are conformationally flexible in solution.^[11,20] This is a result of the loss of macrocyclic aromaticity combined with the constraint generated by the introduction of pyridine. However, it has been noticed that the H(22) resonances of **2**-M and **10**-M are in unusually downfield positions { δ H(22) = 8.81 **2**-M; 8.30 **10**-M ppm, [D]chloroform, 298 K}. Thus, the replacement of the 6,21-phenyl groups by mesityl substituents results in a downfield relocation of the H(22) resonances of **2**-M and **10**-M (1.0 and 0.6 ppm with respect to **2** and **10**, respectively). These changes are accompanied by a rather modest upfield relocation of the H(8/19) resonances, which approach the position of the H(9/18) counterparts, suggesting that these β -H hydrogen atoms acquire a similar orientation with respect to the shielding zones of the adjacent *meso*-aryl groups. The effectively orthogonal position of the *meso*-phenyl groups removes the source of shift difference for the H(8/19) and H(9/18) resonances seen for **2** and **10**. Clearly, the detected spectroscopic changes have been triggered by introduction of the bulky mesityl substituents at the 6- and 21-positions, as they are primarily visible at the adjacent molecular fragments.

Structural Studies

X-ray analyses have been performed for compounds **2** and **10**. The molecular structure of **2** is visualized in Figure 3.

The pyridine ring is sharply tipped out of the N(23)N(24)N(25) plane, making room for the 6,21-phenyl groups, which are almost coplanar with the macrocycle. An angle between the pyridine mean plane and the plane of N(23)N(24)N(25) atoms equals 39.8(1)°. π -Bonds within the tripyrrane subunit are largely localized in the manner indicated by the valence structure of **2**. On the other hand, the bond lengths in the six-membered ring are pyridine-like: C(1)–C(2) 1.413(2), C(2)–N(3) 1.329(2), N(3)–C(4) 1.337(2), C(4)–C(5) 1.403(2), C(1)–C(22) 1.393(3), C(5)–C(22) 1.393(3) Å. The C(21)–C(1) and C(5)–C(6) distances [1.459(2) Å and 1.465(2) Å] approach the single-bond limit for C(sp²)–C(sp²). These structural features confirm that the six-membered ring incorporated in the framework of **2**

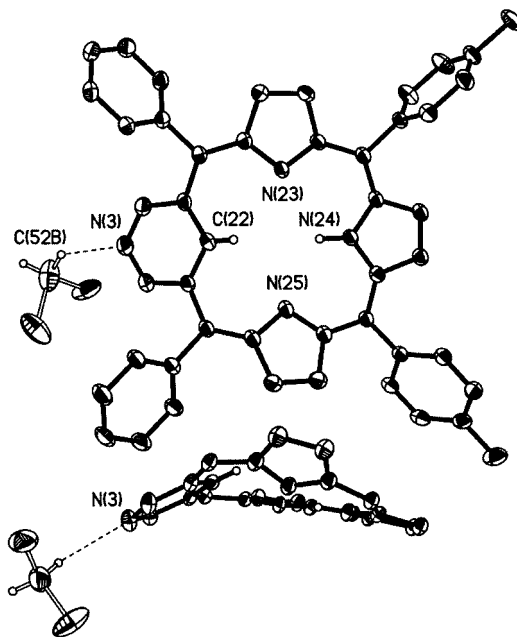


Figure 3. Molecular structure of **2** (top: perspective view, bottom: side view). Perimeter hydrogen atoms and *meso*-aryl groups omitted for clarity. The hydrogen bond between the dichloromethane molecule (the most abundant occupation) and the perimeter nitrogen atom is shown in both projections. Thermal ellipsoids are at the 50% probability level.

completely blocks macrocyclic delocalization while retaining unperturbed pyridine aromaticity.

Figure 4 shows the molecular structure of **10**. The fundamental structural features of **2** have been preserved in the structure of **10**. In particular the macrocyclic ring is puckered and the angle between the pyridine mean plane and the plane of N(23)S(24)N(25) atoms equals 42.6(1)°. There is an appreciable effect of the conjugation on the thiophene fragment. The bond lengths within the thiophene ring are altered. Thus, the C _{α} –C _{β} bonds [1.447(3), 1.442(3) Å] are longer than the C _{β} –C _{β} distances [1.347(3) Å] whereas the reverse is true for thiophene^[38] and tetrathiaporphyrinogen.^[39] The C _{α} –S bond lengths of 1.750(2) and 1.756(2) Å remain practically unchanged. The C(11)–C(12) [1.378(3) Å] and C(15)–C(16) [1.382(3) Å] distances reflect some double-bond character in the bonds that link the thiophene ring to the macrocyclic frame.

In the crystal lattice of **2** the pyridine nitrogen atom N(3) is adjacent to the molecule of dichloromethane, which forms a weak hydrogen bond C–H \cdots N(3) for each of the three disordered orientations. The C–H \cdots N(3) distances equal 2.41 (156°), 2.52 (140°), 2.40 Å (124°), respectively [the appropriate C–H \cdots N(3) angle is given in parentheses]. The analogous interaction has been observed in the crystal of **10** where the C–H \cdots N(3) distances equal 2.30 (149°), 2.69 (155°), and 2.55 Å (168°). The C–H \cdots N(3) structural characteristics in **2** and **10** are comparable to other cases of C–H \cdots N hydrogen bonds, where the pyridine nitrogen atom is involved.^[40,41]

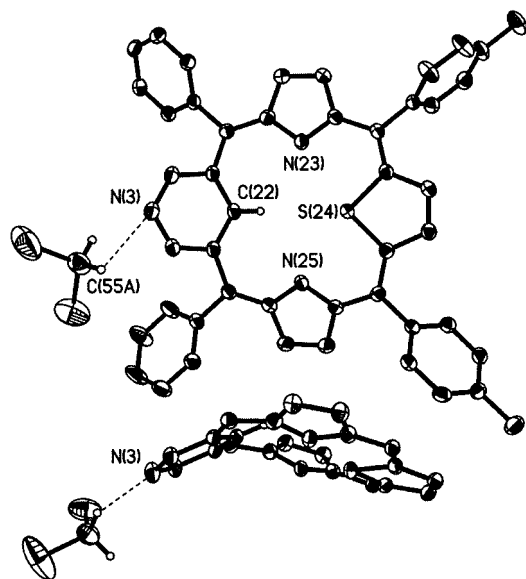


Figure 4. Molecular structure of **10** (top: perspective view, bottom: side view). Perimeter hydrogen atoms and *meso*-aryl groups omitted for clarity. The hydrogen bond between the dichloromethane molecule (the most abundant occupation) and the perimeter nitrogen atom is shown in both projections. Thermal ellipsoids are at the 50% probability level.

Titration of **2** with TFA

The ^1H NMR spectroscopic titration of **2** with trifluoroacetic acid (TFA) has been carried out in $[\text{D}_2]$ dichloromethane at 203 K (Figure 5). The individual resonances of neutral **2** and two dicationic species $2'\text{-H}_2$ and $2''\text{-H}_2$ (Scheme 6) have been identified one after the other during the ^1H NMR titration. Eventually, at the highest concentration of TFA at 183 K the tricationic form 2-H_3 has been detected. These observations have been attributed to a slow exchange among the detected ionic forms at 203 K. The unambiguous assignments of resonances have been obtained by 2D ^1H NMR COSY and NOESY spectroscopic experiments. The protonation mechanism was originally analyzed based on the well-separated set of NH singlets in the $\delta = 9\text{--}18$ ppm spectral region to be correlated with the spectroscopic pattern of pyridine and $\beta\text{-H}$ resonances located at the $\delta = 9\text{--}6$ ppm region.

The general mechanism of protonation, which includes the considered tautomeric species, is presented in Scheme 6. The very first protonation step concerns the basic nitrogen atoms of the macrocyclic core (see below). Thus, the number of resonances, contained in individual H(2/4), H(22), $\beta\text{-H}$ and NH sets indicate unambiguously the number of the species formed in the particular stage of the titration. Their multiplicity and relative NH intensities could be discussed in structural terms. We have already shown that the neutral form is protonated at the 24(NH) position ($\delta = 10.07$ ppm, 203 K). Hypothetically one can predict the formation of two tautomers at a monocationic level (Scheme 6): $[\text{NH}(23), \text{N}(24), \text{NH}(25)]$; $[\text{NH}(23), \text{NH}(24), \text{N}(25)]$.

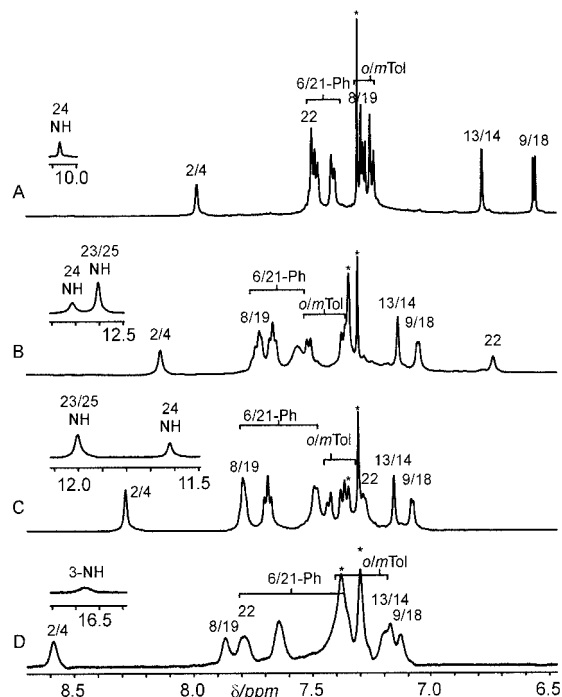
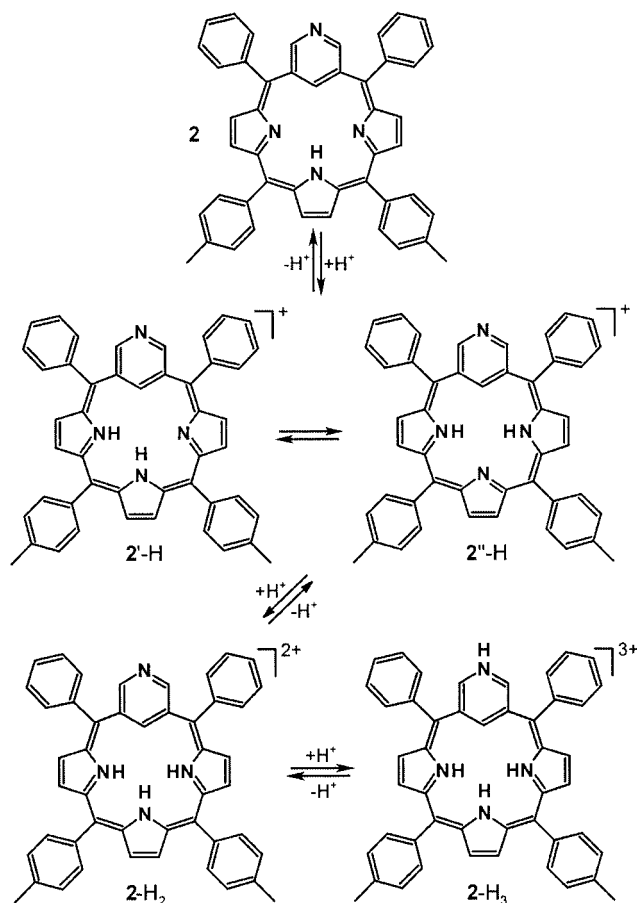


Figure 5. ^1H NMR spectra (downfield regions presented): (A) **2** (203 K), (B) $2'\text{-H}_2$ (203 K), (C) $2''\text{-H}_2$ (203 K), (D) 2-H_3 (183 K) as obtained during the course of titration of **2** with TFA in $[\text{D}_2]$ -dichloromethane. NH resonances are shown in the associated insets. The inner NH resonances of 2-H_3 at $\delta = 10.97$ and 11.72 ppm, overlapped with the COOH resonance of TFA, are not shown in trace D. Resonance assignments follow the numbering given in Scheme 1.

Thus, the monocation $2'\text{-H}$ is expected to demonstrate two NH resonances (intensity ratio 1:1). Alternatively, one NH resonance but with a relative intensity of two hydrogen atoms should be detected for $2''\text{-H}$. However, instead of a monocationic pattern the very first addition of TFA provides the ^1H NMR spectroscopic features readily assigned to a dication $2'\text{-H}_2$. This dication demonstrates two NH resonances of the predictable, because of symmetry, 2:1 intensity ratio. The appropriate scalar couplings NH(23/25)–H(8/19), NH(23/25)–H(9/18) and NH(24)–H(12/13) have been detected in the COSY spectra of $2'\text{-H}_2$, unambiguously confirming the complete protonation of the pyrrole nitrogen atoms. The further stepwise addition of TFA results in the gradual increase of the $2''\text{-H}_2$ concentration accompanied by the parallel intensity loss of $2'\text{-H}_2$. In particular, the second set of two NH singlets has been detected at higher TFA concentrations. The spectral pattern (Figure 5, trace C) corresponds to the dication ($2''\text{-H}_2$) because the protonation status of the inner nitrogen atoms remains intact, considering the relative intensity of resonances (2:1) and scalar couplings to the appropriate β -hydrogen atoms. Thus, it is important to realize that the ^1H NMR spectral changes require at least two different dications in equilibrium. Presumably, the process involves two tight ionic aggregates $\{[2\text{-H}_2](\text{CF}_3\text{COO})\}^+$ and $\{[2\text{-H}_2](\text{CF}_3\text{COO})_2\}$.

The considerable difference of the NH shifts for two dications most probably results from the steric requirements

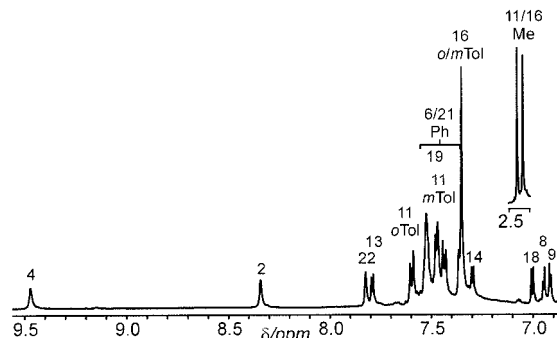
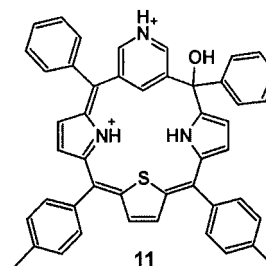
Scheme 6. Protonation of **2**.

imposed by monocoordinate (one TFA ligand bound above the porphyrin plane) and dicoordinate arrangements (two TFA ligands on the opposite side of the porphyrin plane). The contribution of the NH hydrogen atom in the network of hydrogen bonds, which involve CF_3COO^- and CF_3COOH , offers the other factor, which substantially changes the NH chemical shift. Actually, the dications of 6,11,16,21-tetraaryl-3-aza-*m*-benzporphyrin **2-H₂** behave as other polyprotonated macrocyclic cationic ligands,^[42] including extended porphyrins,^[1,43] which are known for their selective interactions with inorganic and organic anions. The coordination of TFA by the 2-methyl-5,10,15,20-tetra-phenyl-2-aza-21-carbaporphyrin,^[44] and 5,10,15,20-tetra-arylporphyrin dications have been described previously.^[45]

The additional equilibria, which are reflected by the smooth change of chemical shifts for **2''-H₂**, also suggest the independent interaction of this ionic aggregate with the bulk of TFA through a network of hydrogen bonds. The last protonation step, set off by the large molar excess of TFA, yielded the trication **2-H₃**. This protonation engages the perimeter nitrogen atom of pyridine. Significantly, the pyridinium N(3)H resonance has been directly identified at the unique position $\delta = 16.56$ ppm (183 K). The detected scalar couplings (COSY) N(3)H–H(2/4) confirmed the protonation at this particular position.

Formation of 6-Hydroxy-3-aza-*m*-benziphlorin (**11**)

In contrast to 6,21-diphenyl-11,16-di-*p*-tolyl-3-aza-*m*-benzporphyrin (**2**), where the protonations of basic nitrogen atoms have been solely detected, the reaction of 6,21-diphenyl-11,16-di-*p*-tolyl-24-thia-3-aza-*m*-benzporphyrin (**10**) with TFA includes a profound modification of the macrocycle (Figure 6, Scheme 7).

Figure 6. ¹H NMR spectrum of **11** ($[\text{D}_2]$ dichloromethane, 203 K). Resonance assignments follow the numbering given in Scheme 1.Scheme 7. Structure of **11**.

Formally, the reaction can be classified as an addition of water to **10** to produce 6-hydroxy-6,21-diphenyl-11,16-di-*p*-tolyl-3-aza-*m*-benziphlorin (**11**), which structurally resembles porphyrin-derived phlorins and is analogous to alkyl-substituted benziphlorin and pyrriphlorin.^[8,22]

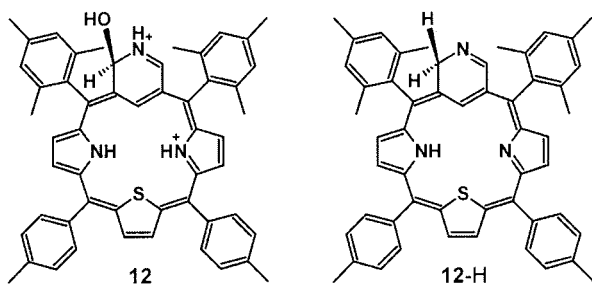
Previously, we have also shown that the reaction of **1** with water or methanol yields 6-hydroxy-6,11,16,21-tetra-phenylbenziphlorin and 6-methoxy-6,11,16,21-tetra-phenylbenziphlorin.^[10] This reactivity resembles the nucleophilic *meso* addition of hydride or hydroxide to $(\text{TPP})\text{Au}^{\text{III}}\text{Cl}$ to yield phlorin or hydroxyphlorin complexes.^[46]

The reaction is regioselective since only saturation at the 6-position was observed. The ¹H NMR spectrum reflects symmetry lowering of **11** in comparison to **2** (Figure 6). In particular, the two pyrrolic ($\delta = 7.79/7.29$ and $6.95/6.91$ ppm) and one thiophenic ($\delta = 7.48/7.00$ ppm) AB patterns have been identified ($[\text{D}_2]$ dichloromethane, 203 K). The C(6) carbon atom of **11** produces a resonance at $\delta = 77.0$ ppm, which is consistent with its tetrahedral geometry. Analogously, the addition of ethanol to **10** yielded 6-ethoxy-6,21-diphenyl-11,16-di-*p*-tolyl-3-aza-*m*-benziphlorin (**11-OEt**). The diagnostic set of two complex multiplets at $\delta = 3.25$ and 3.19 ppm ($[\text{D}]$ chloroform, 298 K) has been assigned to the ethoxy methylene group. The difference in the chemical shifts detected for the two methylene

multiplets is due to the diastereotopic effect as the chirality center is created at the tetrahedrally hybridized C(6) atom. Addition of triethylamine to **11** resulted in the quantitative recovery of **10**. The easy accessibility of phlorin **11** is related to the loss of aromaticity incurred by **10**.

Formation of 2-Hydroxy-24-thia-3-aza-*m*-benzichlorin (**12**)

The titration of 6,21-dimesityl-11,16-di-*p*-tolyl-24-thia-3-aza-*m*-benzporphyrin (**10-M**) (203 K, [D₂]dichloromethane) with TFA reveals the changes in resonance positions, which correspond to the regular nitrogen protonation of 24-thia-3-aza-*m*-benzporphyrin. However, the severe broadening of all resonances assigned to protonated species, observed even at 183 K, ruled out a detailed analysis of ionic structures. The protonation initiates an addition of the water molecule, which yields the aromatic 2-hydroxy-6,21-dimesityl-11,16-di-*p*-tolyl-24-thia-3-aza-*m*-benzichlorin (**12**) (Scheme 8). Actually, such a route is preferred at 298 K, where **10-M** converts into **12** after addition of TFA, dichloroacetic acid or HCl_(g). The large amount of triethylamine enables the quantitative recovery of **12** into **10-M**.



Scheme 8. Structure of **12**.

The complete assignments of all ¹H NMR resonances for **12** are shown in Figure 7. All pyrrole resonances $\delta = 8.22/8.21$ [AB, ³*J*(H,H) = 4.6 Hz], $8.02/7.97$ [AB, ³*J*(H,H) = 4.8 Hz] and thiophene resonances $\delta = 9.23/9.20$ ppm [AB, ³*J*(H,H) = 5 Hz] are shifted downfield ([D]chloroform, 298 K). The strongly upfield position of the H(22) signal [$\delta = -3.36$ ppm, ⁴*J*(H,H) = 1.8 Hz], scalar-coupled with the downfield shifted H(4) signal ($\delta = 9.53$ ppm) are readily accounted for by the aromatic ring-current effect. The structurally informative H(2) resonance was identified at $\delta = 6.74$ ppm. The ¹³C chemical shift of C(2) ($\delta = 76.8$ ppm) is consistent with the tetrahedral hybridization. The fully protonated **12** (solution saturated with HCl) demonstrated three NH resonances at $\delta = 16.2$, 1.75, and 1.80 ppm readily assigned to the perimeter and inner core localizations.

Addition of ethanol to **10-M** in the presence of dichloroacetic acid afforded 2-ethoxy-6,21-dimesityl-11,16-di-*p*-tolyl-24-thia-3-aza-*m*-benzichlorin (**12-OEt**). The diagnostic set of two complex multiplets at $\delta = 3.46$ and 3.02 ppm have been assigned to the ethoxy methylene group. The strong difference in the chemical shifts detected for the two methylene multiplets is due to the diastereotopic effect as the chirality center is created on the tetrahedrally hybridized C(2) atom.

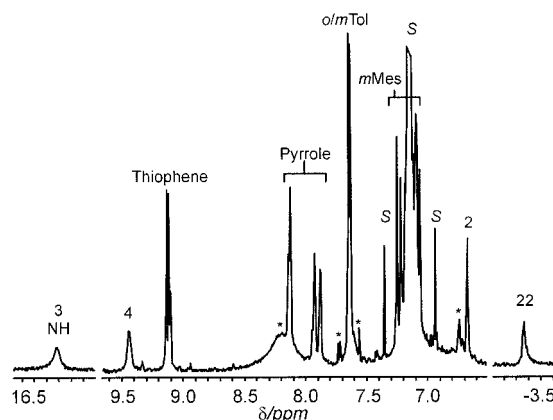


Figure 7. ¹H NMR spectrum (selected downfield regions presented) of **12** ([D]chloroform, HCl_(g), 203 K).

Mechanistically, the formation of **12** can be considered as an alternate route to an acid-initiated addition of water to 24-thia-3-aza-*m*-benzporphyrins. The formation of phlorin seems to be characteristic of **10**. In spite of the obvious structural similarities, the replacement of *meso*-phenyl groups in **10** by *meso*-mesityl groups in **10-M** redirects the hydroxy anion addition to the pyridine moiety to form **12**. Clearly, the steric hindrance of mesityl groups limits the access at the 6-position, which is preferable for **10**. Thus, **10-M** yielded the new aromatic macrocycle by initial protonation, followed by an addition of the hydroxy group at C(2). In the course of this reversible process the trigonal to tetrahedral rearrangements originate at the C(2) atom but their consequences are extended to the whole structure allowing the aromatic conjugation. The trapped carbaporphyrinoid **12** is structurally related to the hypothetical **12-H** (Scheme 8) as both contain an identical macrocyclic frame. In this same line, the macrocycles **10-M** and **12-H** are mutually convertible by a hydrogenation/dehydrogenation step presuming that the addition of two hydrogen atoms is localized at the C(2) and one of the internal nitrogen atoms.

Conclusion

The targeted 6,11,16,21-tetraaryl-3-aza-*m*-benzporphyrin **2** and 6,11,16,21-tetraaryl-21-thia-3-aza-*m*-benzporphyrin **10** contain a (C₃NN) or (C₃NS) coordination core of carbaporphyrinoids. Significantly, the nitrogen atom at the macrocyclic perimeter provides some means to control overall macrocyclic properties by protonation or alkylation. Potentially, an external *N*-coordination of pyridine offers a route to construct polymetallic arrays where the pyridine moiety will serve as a unique bridge, which links two metal ions involving a simultaneous coordination by C- and N-ends. The flexibility of macrocyclic structures, discovered in the course of protonation studies, leads to alternative, non-conventional routes to modify complex molecular arrays.

Experimental Section

Instrumentation: NMR spectra were recorded with a Bruker Avance 500 spectrometer (base frequencies: 500.13 MHz ^1H , 125.77 MHz ^{13}C). Spectra were referenced to the residual solvent signals. Assignments of ^1H NMR spectra were obtained from COSY and NOESY maps, and ^{13}C NMR spectra were based on ^1H - ^{13}C HMQC and HMBC experiments. Absorption spectra were recorded with a diode-array Hewlett Packard 8453 spectrometer. Mass spectra were recorded with an AD-604 spectrometer using the electron impact and liquid matrix secondary ion mass spectrometry techniques.

Materials: 3,5-Dibromopyridine, *n*-butyllithium, mesitaldehyde and mesyl chloride (from Aldrich) were used as received. Chloroform (stabilized with amylene) was received from AppliChem. Basic alumina (Aldrich or Alfa-Aesar) was deactivated before chromatography. 2,5-Bis[hydroxy(*p*-tolyl)methyl]thiophene (**9**) was obtained as described in the literature.^[47]

3,5-Bis[hydroxy(phenyl)methyl]pyridine (4; 4-M): *n*BuLi (15.9 mL of 1.6 M solution in hexanes, 24.55 mmol) was added to a dry THF solution of 3,5-dibromopyridine (3 g, 12.66 mmol, $-100\text{ }^\circ\text{C}$). The resulting mixture was stirred at $-100\text{ }^\circ\text{C}$ for 0.5 h. Benzaldehyde (2.6 mL, distilled; or 3.75 mL of mesitaldehyde for **4-M**) was then added and the reaction mixture was left for several hours while the cooling bath reached room temperature. The solvents were evaporated under reduced pressure. In the case of **4** the foam that had formed was dissolved in 20% H_2SO_4 (150 mL) and washed four times with CH_2Cl_2 (25 mL). The acid layer was neutralized with K_2CO_3 , and the product was extracted several times with CH_2Cl_2 (25 mL). The combined solutions were dried with MgSO_4 and filtered. The solvents were evaporated under reduced pressure. The residue was dissolved in CH_2Cl_2 and chromatographed on a grade III basic alumina column. The fraction eluted with $\text{CH}_2\text{Cl}_2/\text{CH}_3\text{OH}$ (85:15, v/v) was collected, and the solvent was removed with a vacuum rotary evaporator to give **4** as the yellow foam. An essential modification of the procedure was necessary to separate **4-M**. The foam was dissolved in 20% H_2SO_4 (50 mL) and CH_2Cl_2 (50 mL). Both layers were transferred into a beaker and diluted with water (400 mL). The solution was neutralized by addition of K_2CO_3 (with vigorous stirring) and separated. The solution was extracted several times with CH_2Cl_2 (25 mL), dried with MgSO_4 , filtered, and the solvent removed with a vacuum rotary evaporator. The residue was dissolved in CH_2Cl_2 and chromatographed on a grade II basic alumina column and **4-M** was eluted with $\text{CH}_2\text{Cl}_2/\text{CH}_3\text{OH}$ (95:5, v/v). Yields: **4**: 1.7 g (46%); **4-M**: 950 mg (20%). **4**: ^1H NMR (CDCl_3 , 298 K): δ = 8.43 [d, $^4J(\text{H,H})$ = 2.2 Hz, 2 H, 2/6-pyridine], 7.75 [t, $^4J(\text{H,H})$ = 2.2 Hz, 1 H, 4-pyridine], 7.35–7.25 (10 H, Ph), 5.85, 2.40 (s, *CHOH*, *CHOH*) ppm. ^{13}C NMR (CDCl_3 , 298 K): δ = 147.1 (2/6-pyridine), 143.0 (1-Ph), 139.6 (3/5-pyridine), 132.8 (4-pyridine), 128.9, 128.1, 126.7 (2/3/4-Ph), 74.1 (methine) ppm. MS (ESI): m/z = 291. **4-M**: ^1H NMR (CDCl_3 , 298 K, mixture of stereoisomers): δ = 8.11 (2 H, 2/6-pyridine), 7.76 (1 H, 4-pyridine), 6.79 (4 H, *m*-Mes), 6.26, (2 H, *CHOH*), 2.80 (2 H, *CHOH*), 2.24 (6 H, Me-4'), 2.15 (12 H, Me-2') ppm. ^{13}C NMR (CDCl_3 , 298 K, mixture of stereoisomers): δ = 145.5 (2/6-pyridine), 138.5 (3/5-pyridine), 137.8 (4-Mes), 136.9, 135.8 (1/2-Mes), 131.1 (4-pyridine), 130.3 (3-Mes), 69.4 (methine), 21.7 (Me-2'), 21.0 (Me-4') ppm. MS (ESI): m/z = 390.

3,5-Bis[phenyl(2-pyrrolyl)methyl]pyridine (7): Mesyl chloride (325 μL , 2.1 equiv. in 500 mL of CHCl_3) was added dropwise (2 h) to the solution of **4** (582 mg, 2 mmol) and triethylamine (585 μL , 2.1 equiv.) in CHCl_3 under nitrogen at $0\text{ }^\circ\text{C}$. Subsequently, the reaction mixture was refrigerated for 3 d. After this time, the solvent

was removed in vacuo. The residue was dissolved in 5 mL of pyrrole and the reaction mixture, protected from light, was stirred under nitrogen for 3 d. The reaction was quenched by addition of CH_2Cl_2 (50 mL). The resulting solution was washed with 10% H_2SO_4 ($6 \times 10\text{ mL}$) and water. The solution was neutralized by addition of K_2CO_3 until the liberation of CO_2 had ceased, extracted with CH_2Cl_2 several times and dried with MgSO_4 , filtered, and the solvent removed with a vacuum rotary evaporator. The excess of pyrrole was removed in a vacuum line. The dark residue was chromatographed on a grade II basic alumina column. The product was eluted with $\text{CH}_2\text{Cl}_2/\text{CH}_3\text{OH}$ (99.8:0.2, v/v) and the solvent was evaporated. Yield: 350 mg (45%). ^1H NMR (CDCl_3 , 298 K, mixture of stereoisomers): δ = 8.30 (2 H, 2/6-pyridine), 7.79 (2 H, NH), 7.35 (1 H, 4-pyridine), 7.29–7.10 (10 H, Ph); pyrrole: δ = 6.68 (2 H), 6.11 (2 H), 5.71 (2 H), 5.40 (2 H, methine) ppm. ^{13}C NMR (CDCl_3 , 298 K): δ = 148.6 (2/6-pyridine), 142.0 (1-Ph), 138.5 (3/5-pyridine), 136.8 (4-pyridine), 132.5 (2-pyrrole), 128.93, 128.87, 127.3 (2/3/4-Ph), 117.8 (5-pyrrole), 108.6 (4-pyrrole), 108.4 (3-pyrrole), 48.3 (methine) ppm. MS (ESI): m/z = 377.

7-M: The synthetic procedure followed that of **7** until the excess pyrrole was removed. The black residue was dissolved in CH_2Cl_2 and *n*-hexane was added. The volume was reduced. The yellow solution of **7-M** was decanted. The procedure was repeated several times. The solutions were combined and the solvent was removed with a vacuum rotary evaporator. Yield: 852 mg (90%). ^1H NMR (CDCl_3 , 298 K, mixture of stereoisomers): δ = 8.33 (2 H, 2/6-pyridine), 7.76 (2 H, NH), 7.36 (1 H, 4-pyridine), 6.80 (4 H, *m*-Mes); pyrroles: δ = 6.80 (2 H), 6.62 (2 H), 6.10 (2 H), 5.52 (2 H, methine), 2.26 (6-H, Me-4'), 1.96 (12-H, Me-2') ppm. ^{13}C NMR (CDCl_3 , 298 K, mixture of stereoisomers): δ = 148.4 (2/6-pyridine), 136.2 (3/5-pyridine), 136.6 (4-pyridine), 137.6 (1-Mes), 136.9 (4-Mes), 134.4 (2-Mes), 132.0 (1-pyrrole), 130.6 (3-Mes), 116.9 (5-pyrrole), 108.5 (4-pyrrole), 107.3 (3-pyrrole), 42.6 (methine), 21.1 (Me-2'), 21.0 (Me-4') ppm. MS (ESI): m/z = 474.

6,21-Diphenyl-11,16-di-*p*-tolyl-3-aza-*m*-benzporphyrin (2): 3,5-bis[phenyl(2-pyrrolyl)methyl]pyridine (**7**) (195 mg, 0.5 mmol), pyrrole (35 μL , 0.5 mmol), and *p*-tolualdehyde (355 mL, 3 mmol) were added to dry CH_2Cl_2 (500 mL) under nitrogen. TFA (300 μL , 3.9 mmol) was added and the reaction mixture was protected from light and stirred for 1 h. The reaction mixture was neutralized with 560 μL (4 mmol) of triethylamine. DDQ (357 mg, 1.58 mmol) was subsequently added and the mixture was stirred for several minutes, and evaporated under reduced pressure. The residue is subjected to chromatography (grade II basic alumina, CH_2Cl_2). The desired product eluted as a green band following a trace of (TTP) H_2 . Recrystallization from $\text{CH}_2\text{Cl}_2/n$ -hexane yielded deep green crystals. Yield: 8.1 mg (2.5%). ^1H NMR (CDCl_3 , 298 K): δ = 10.36 [s, 1 H, NH(24)], 8.12, 7.80 [A_2B , (2 + 1) H, $^4J(\text{H,H})$ = 2.06 Hz, H(2/4), H(22)], 7.41–7.47 (m, 10 H, Ph), 7.32, 7.23 [A_2B_2 , (2 \times 2) H, $^3J(\text{H,H})$ = 8.02, *olm*-Tol], 7.19 [AB, 2 H, $^3J(\text{H,H})$ = 4.81 Hz, H(8/19)], 6.73 [s, 2 H, H(13/14)], 6.57 [AB, 2 H, $^3J(\text{H,H})$ = 4.81 Hz, H(9/18)], 2.42 (s, 6 H, *p*-Tol) ppm. ^{13}C NMR (CDCl_3 , 298 K): δ = 172.7 (10/17), 158.0 (7/20), 152.1 (2/4), 148.3 (12/15), 141.7, 140.8, 132.4 (4-Tol), 136.5 (8/19), 136.4, 133.2 (1-Tol) 133.1 (Ph), 132.1 (2-Tol), 131.4 (9/18), 130.2 (13/14), 128.74 (Ph), 128.67 (3-Tol), 127.6 (Ph), 115.6, 115.2 (22), 21.4 (*p*-Me) ppm. UV/Vis (CH_2Cl_2): λ_{max} (log ϵ) = 322 (4.48), 411 (4.75), 730 nm (very broad, 3.99). HRMS (ESI): m/z = 655.2880 (655.2861 for [$\text{C}_{47}\text{H}_{34}\text{N}_4 + \text{H}$] $^+$).

6,21-Dimesityl-11,16-di-*p*-tolyl-3-aza-*m*-benzporphyrin (2-M): **2-M** was obtained analogously to **2**, with **7-M** replacing **7**. The condensation reaction took 4 h. Yield after the $\text{CH}_2\text{Cl}_2/\text{CH}_3\text{OH}$ crystallization: 55.5 mg (15%). ^1H NMR (CDCl_3 , 298 K): δ = 10.43 [s,

1 H, NH(24)], 8.81, 8.30 [AB₂, (2 + 1) H, ⁴J(H,H) = 2.06 Hz, H(2/4), H(22)], 7.30, 7.21 [A₂B₂, (2 × 2) H, ³J(H,H) = 7.79 Hz, *o/m*-Tol], 6.92 (s, 4 H, *m*-Mes), 6.78 [AB, 2 H, ³J(H,H) = 4.81 Hz, H(8/19)], 6.67 [s, 2 H, H(13/14)], 6.57 (AB, 2 H, ³J(H,H) = 4.81 Hz, H(9/18)], 2.42 (s, 6 H, *p*-Tol), 2.35 (s, 6 H, Me-4'), 1.99 (s, 12 H, Me-2') ppm. ¹³C NMR (CDCl₃, 298 K): δ = 172.1 (10/17), 158.8 (7/20), 152.8 (2/4), 138.1 (1/5), 137.8 (4-Mes), 137.63 (2-Mes), 137.57 (1-Mes), 137.4 (4-Tol), 136.63 (9/18), 136.57 (1-Tol), 132.0 (2-Tol), 131.4 (8/19), 131.1 (6/21), 130.0 (13/14), 128.8 (3-Tol), 128.0 (3-Mes), 123.2 (22), 115.3 (11/16), 21.5, (*p*-Tol) 21.3 (Me-2'), 20.9 (Me-4') ppm. UV/Vis (CH₂Cl₂): λ_{max} (log ε) = 325 (4.60), 410 (4.68), 730 nm (very broad, 3.94).

6,21-Diphenyl-11,16-di-*p*-tolyl-24-thia-3-aza-*m*-benzporphyrin (10): Compound **10** was obtained analogously to **2** but in place of pyrrole and aldehyde, 2,5-bis[hydroxyl(*p*-tolyl)methyl]thiophene (**9**) (162 mg, 0.5 mmol) was used. Yield: 10 mg (3%). ¹H NMR (CDCl₃, 298 K): δ = 8.20, 7.70 [A₂B, (2 + 1) H, ⁴J(H,H) = 2.06 Hz, H(2/4), H(22)], 7.47–7.38 (m, 10 H, Ph), 7.33, 7.26 [A₂B₂, (2 × 2) H, ³J(H,H) = 8.02, *o/m*-Tol], 7.28 [AB, 2 H, ³J(H,H) = 4.58 Hz, H(8/19)], 7.18 [s, 2 H, H(13/14)], 6.66 [AB, 2 H, ³J(H,H) = 4.58 Hz, H(9/18)], 2.42 (s, 6 H, *p*-Tol). ¹³C NMR (CD₂Cl₂, 298 K): δ = 172.7 (10/17), 156.2 (7/20), 154.9 (12/15), 152.4 (2/4), 143.9 (6/21), 142.2 (1-Ph), 138.2 (4-Tol), 136.9 (8/19), 136.1 (13/14), 135.8, 135.1, 133.0 (Ph), 131.3 (2-Tol), 130.7 (9/18), 130.1 (3-Tol), 129.4 (Ph), 129.3, 128.2 (Ph), 119.4 (22), 21.4 (Me) ppm. UV/Vis (CH₂Cl₂): λ_{max} (log ε) = 319 (4.37), 352 (4.34), 412 (4.65), 661 nm (3.98). HRMS (ESI): *m/z* = 672.2496 (672.2473 for [C₄₇H₃₃N₃S+H]⁺).

6,21-Dimesityl-11,16-di-*p*-tolyl-24-thia-3-aza-*m*-benzporphyrin (10-M): **10-M** was obtained analogously to **2-M** but in place of pyrrole and aldehyde 2,5-bis[hydroxyl(*p*-tolyl)methyl]thiophene (**9**) (162 mg, 0.5 mmol) was used. Yield: 68 mg (18%). ¹H NMR (CDCl₃, 298 K): δ = 8.35, 8.30 [A₂B, (2 + 1) H, ⁴J(H,H) = 2.13 Hz, H(2/4), H(22)], 7.35, 7.21 [A₂B₂, (2 × 2) H, ³J(H,H) = 8.03 Hz, *o/m*-Tol], 7.21 [s, 2 H, H(13/14)], 6.93 (s, 4 H, *m*-Mes), 6.87, 6.61 [AB, (2 × 2) H, ³J(H,H) = 4.72 Hz, H(9/18), H(8/19)], 2.42 (s, 6 H, *p*-Tol), 2.36 (s, 6 H, Me-4'), 1.99 (s, 12 H, Me-2') ppm. ¹³C NMR (CDCl₃, 298 K): δ = 172.5 (10/17), 156.7 (7/20), 154.9 (12/15), 152.8 (2/4), 141.6 (6/21), 138.1 (4-Mes), 138.0 (Mes), 137.7 (4-Tol), 137.3 (2-Mes), 137.1 (8/19), 136.0 (13/14), 135.7 (1-Tol), 132.7 (1/5), 131.1 (2-Tol), 130.2 (9/18), 129.9 (11/16), 129.1 (3-Tol), 128.3 (3-Mes), 123.6 (22), 21.5 (*p*-Tol), 21.3 (Me-4'), 20.9 (Me-2') ppm. UV/Vis (CH₂Cl₂): λ_{max} (log ε) = 323 (4.59), 412 (4.66), 655 nm (4.01). HRMS (ESI): *m/z* = 756.3456 (756.3412 for [C₅₃H₄₅N₃S + H]⁺).

X-ray Data Collection and Refinement: Crystals of **2** and **10** were prepared by diffusion of *n*-hexane into a CH₂Cl₂ solution contained in a thin tube (4 °C). Data collection: The measurement of **2** was performed with an Oxford Diffraction KM4 Xcalibur PX κ-geometry diffractometer using Mo-*K*_α radiation (λ = 0.71073 Å), *T* = 100 K, in the ω-scan mode, 2θ_{max} = 72.36°; the measurement of **10** was performed with an Oxford Diffraction KM4 CCD κ-geometry diffractometer using Mo-*K*_α radiation (λ = 0.71073 Å), *T* = 100 K, in the ω-scan mode, 2θ_{max} = 56.92°. The structures were solved by using direct methods with SHELXS-97 and refined against |*F*²| using SHELXL-97 (G. M. Sheldrick, University of

Table 1. Crystal data for **2** and **10** with refinement details.

Compound	2	10
Crystals grown by	slow diffusion of <i>n</i> -hexane into CH ₂ Cl ₂ solution	slow diffusion of <i>n</i> -hexane into CH ₂ Cl ₂ solution
Crystal habit	dark green plate	dark green plate
Crystal size [mm]	0.4 × 0.2 × 0.1	0.8 × 0.5 × 0.4
Empirical formula	C ₄₇ H ₃₄ N ₄ ·CH ₂ Cl ₂	C ₄₇ H ₃₃ N ₃ S·CH ₂ Cl ₂
Formula mass	739.71	756.75
<i>a</i> [Å]	10.205(3)	10.311(3)
<i>b</i> [Å]	13.074(3)	12.935(3)
<i>c</i> [Å]	14.236(3)	14.395(3)
<i>α</i> [°]	82.55(3)	82.41(3)
<i>β</i> [°]	84.24(3)	88.03(3)
<i>γ</i> [°]	82.84(3)	82.84(3)
<i>V</i> [Å ³]	1861.8(8)	1887.9(8)
<i>Z</i>	2	2
<i>d</i> _{calcd} [g cm ⁻³]	1.319	1.331
Crystal system	triclinic	triclinic
Space group	<i>P</i> $\bar{1}$	<i>P</i> $\bar{1}$
<i>μ</i> [mm ⁻¹]	0.216	0.267
Absorption correction	not applied	not applied
<i>T</i> [K]	100(2)	100(2)
Radiation: Mo- <i>K</i> _α [Å]	0.71073	0.71073
<i>θ</i> range [°]	4.68–36.18	2.86–28.46
<i>hkl</i> range	–15 ≤ <i>h</i> ≤ 16 –21 ≤ <i>k</i> ≤ 21 –23 ≤ <i>l</i> ≤ 23	–13 ≤ <i>h</i> ≤ 13 –16 ≤ <i>k</i> ≤ 16 –18 ≤ <i>l</i> ≤ 19
Reflections:		
Measured	42754	20403
Unique [<i>I</i> /2σ(<i>I</i>)]	9826	6493
Parameters/restraints	543/1	539/1
<i>S</i>	1.133	1.087
<i>R</i> ₁ ^[a]	0.0826	0.0585
<i>wR</i> ₂	0.2363	0.1599

$$[a] R_1 = \sum |F_o - F_c| / \sum |F_o|, wR_2 = \{ \sum [w(F_o^2 - F_c^2)^2] / \sum [w(F_o^2)^2] \}^{1/2}.$$

Göttingen, Germany, 1997). For 2 final R_1/wR_2 indices [for $I > 2\sigma(I)$]: 0.0826/0.2363; max./min. residual electron density: +0.42/−0.47 eÅ^{−3}, H atoms except inner H(22) and H(24) were fixed in idealized positions using the riding model constraints. For 10 final R_1/wR_2 indices [for $I > 2\sigma(I)$]: 0.0585/0.1599; max./min. residual electron density: +0.50/−0.45 eÅ^{−3}, H atoms except inner H(22) were fixed in idealized positions using the riding model constraints. A disordered molecule of dichloromethane is present in both structures. Crystal data are compiled in Table 1. CCDC-271579 and -271580 contain the supplementary crystallographic data for this paper. These data can be obtained free of charge from The Cambridge Crystallographic Data Centre via www.ccdc.cam.ac.uk/data_request/cif.

Acknowledgments

Financial support from the Ministry of Scientific Research and Information Technology (Grant 3 T09A 162 28) is kindly acknowledged.

- [1] J. L. Sessler, D. Seidel, *Angew. Chem. Int. Ed.* **2003**, *42*, 5134.
[2] J. L. Sessler, S. J. Weghorn, *Expanded, Contracted, and Isomeric Porphyrins*, Pergamon, New York, 1997.
[3] L. Latos-Grażyński, in: *The Porphyrin Handbook*, vol. 2 (Eds.: K. M. Kadish, K. M. Smith, R. Guilard), Academic Press, New York, 2000, pp. 361–416.
[4] T. D. Lash, *Synlett* **1999**, 279.
[5] T. D. Lash, in: *The Porphyrin Handbook*, vol. 2 (Eds.: K. M. Kadish, K. M. Smith, R. Guilard), Academic Press, San Diego, CA, 2000, pp. 125–199.
[6] M. Stepień, L. Latos-Grażyński, *Acc. Chem. Res.* **2005**, *38*, 88.
[7] A. Srinivasan, H. Furuta, *Acc. Chem. Res.* **2005**, *38*, 10.
[8] K. Berlin, E. Breitmaier, *Angew. Chem. Int. Ed. Engl.* **1994**, *33*, 1246.
[9] T. D. Lash, *Angew. Chem. Int. Ed. Engl.* **1995**, *34*, 2533.
[10] M. Stepień, L. Latos-Grażyński, *Chem. Eur. J.* **2001**, *7*, 5113.
[11] M. Stepień, L. Latos-Grażyński, *J. Am. Chem. Soc.* **2002**, *124*, 3838.
[12] M. Stepień, L. Latos-Grażyński, L. Sztterenber, J. Panek, Z. Latajka, *J. Am. Chem. Soc.* **2004**, *126*, 4566.
[13] H. Furuta, T. Asano, T. Ogawa, *J. Am. Chem. Soc.* **1994**, *116*, 767.
[14] N. Sprutta, L. Latos-Grażyński, *Tetrahedron Lett.* **1999**, *40*, 8457.
[15] N. Sprutta, L. Latos-Grażyński, *Org. Lett.* **2001**, *3*, 1933.
[16] E. Pacholska, L. Latos-Grażyński, L. Sztterenber, Z. Ciunik, *J. Org. Chem.* **2000**, *65*, 8188.
[17] M. Pawlicki, L. Latos-Grażyński, *Chem. Eur. J.* **2003**, *9*, 4650.
[18] P. J. Chmielewski, L. Latos-Grażyński, K. Rachlewicz, T. Głowiak, *Angew. Chem. Int. Ed. Engl.* **1994**, *33*, 779.
[19] M. Stepień, L. Latos-Grażyński, T. D. Lash, L. Sztterenber, *Inorg. Chem.* **2001**, *40*, 6892.
[20] M. Stepień, L. Latos-Grażyński, L. Sztterenber, *Inorg. Chem.* **2004**, *43*, 6654.
[21] C.-H. Hung, F.-C. Chang, C.-Y. Lin, K. Rachlewicz, M. Stepień, L. Latos-Grażyński, G.-H. Lee, S.-M. Peng, *Inorg. Chem.* **2004**, *4118*, 4120.
[22] K. Berlin, E. Breitmaier, *Angew. Chem. Int. Ed. Engl.* **1994**, *33*, 219.
[23] H. J. Callot, E. Schaeffer, *Tetrahedron* **1978**, *34*, 2295.
[24] T. D. Lash, S. T. Chaney, *Chem. Eur. J.* **1996**, *2*, 944.
[25] T. Schönemeier, E. Breitmaier, *Synthesis* **1997**, 273.
[26] T. D. Lash, S. T. Chaney, D. T. Richter, *J. Org. Chem.* **1998**, *63*, 9076.
[27] D. Liu, G. M. Ferrence, T. D. Lash, *J. Org. Chem.* **2004**, *69*, 6079.
[28] T. D. Richter, T. D. Lash, *J. Org. Chem.* **2004**, *69*, 8842.
[29] R. J. P. Corriu, G. Bolin, J. J. E. Moreau, C. Venhet, *J. Chem. Soc., Chem. Commun.* **1991**, 211.
[30] F. H. Carré, R. J. P. Corriu, G. Bolin, J. J. E. Moreau, C. Vernhet, *Organometallics* **1993**, *12*, 2478.
[31] C. R. Adams, R. Bonnett, P. J. Burke, A. Salgado, M. A. Vallés, *J. Chem. Soc., Chem. Commun.* **1993**, 1860.
[32] C. R. Adams, R. Bonnett, P. J. Burke, A. Salgado, M. A. Vallés, *J. Chem. Soc., Perkin Trans. 1* **1997**, 1769.
[33] V. Kral, P. A. Gale, P. Anzenbacher, K. Jursikova, V. Lynch, J. L. Sessler, *Chem. Commun.* **1998**, 9.
[34] W. E. Parham, R. M. Piccirilli, *J. Org. Chem.* **1977**, *42*, 257.
[35] D. Gryko, J. S. Lindsey, *J. Org. Chem.* **2000**, *65*, 2249.
[36] T. D. Lash, *Chem. Eur. J.* **1996**, *2*, 1197.
[37] N. Sprutta, L. Latos-Grażyński, *Chem. Eur. J.* **2001**, *7*, 5099.
[38] W. R. Harsberger, S. H. Bauer, *Acta Crystallogr., Sect. C: Cryst. Struct. Commun.* **1970**, *26*, 1010.
[39] E. Vogel, P. Röhrig, M. Sicken, B. Knipp, A. Herrmann, M. Pohl, H. Schmickler, J. Lex, *Angew. Chem. Int. Ed. Engl.* **1989**, *28*, 1651.
[40] K. Campbell, R. McDonald, M. J. Ferguson, R. R. Tykwinski, *J. Organomet. Chem.* **2003**, *683*, 379.
[41] K. Campbell, R. McDonald, M. J. Ferguson, R. R. Tykwinski, *Organometallics* **2003**, *22*, 1353.
[42] M. Izatt, K. Pawlak, J. S. Bradshaw, R. L. Bruening, *Chem. Rev.* **1991**, *91*, 1721.
[43] J. L. Sessler, P. A. Gale, in: *The Porphyrin Handbook*, vol. 6 (Eds.: K. M. Kadish, K. M. Smith, R. Guilard), Academic Press, San Diego, CA, 2000, pp. 257–278.
[44] P. J. Chmielewski, L. Latos-Grażyński, *J. Chem. Soc., Perkin Trans. 2* **1995**, 503.
[45] M. O. Senge, T. P. Forsyth, L. T. Nguyen, K. M. Smith, *Angew. Chem. Int. Ed. Engl.* **1994**, *33*, 2485.
[46] H. Segawa, R. Azumi, T. Shimidzu, *J. Am. Chem. Soc.* **1992**, *114*, 7564.
[47] A. Ulman, J. Manassen, *J. Chem. Soc., Perkin Trans. 1* **1979**, 1066.

Received: July 6, 2005

Published Online: October 12, 2005